Journal of Materials Chemistry

Dynamic Article Links

Cite this: *J. Mater. Chem.*, 2012, **22**, 4790

www.rsc.org/materials

PAPER

Mussel adhesive protein inspired coatings: a versatile method to fabricate silica films on various surfaces†

Akhilesh Rai and Carole C. Perry

Received 11th November 2011, Accepted 17th January 2012
DOI: 10.1039/c2jm15810h

A simple and versatile biomimetic strategy for the fabrication of silica films on a variety of substrates including gold, polystyrene and silicon wafers was developed using nanogram amounts per cm^2 of silicatein. The strategy exploits the adhesive property of 3,4-dihydroxyphenylalanine (DOPA) and a decapeptide (Ala-Lys-Pro-Ser-Tyr-DHP-Hyp-Thr-DOPA-Lys), important components of mussel adhesive proteins, to modify the surface of substrates. DOPA molecules polymerize to poly(DOPA) and the decapeptide forms thin films on gold substrates at pH 8.5, rendering the substrate compatible for silicatein immobilization. Nearly 50 ng cm^{-2} of silicatein is immobilized on poly(DOPA) and decapeptide coated surfaces where these polymer films act as "cushion" to protect the active structure and maintain the activity of the largely chemically adsorbed silicatein at *ca.* 95% of that experienced in solution. Uniform silica films of thickness 130–140 nm and roughness 12–14.5 nm were fabricated on coated gold surfaces. Evidence to show that this method is also applicable for the fabrication of uniform silica films on polystyrene and silicon substrates over multiple length scales in an economical way is also presented.

Introduction

Silica-based materials especially inorganic–organic hybrid thin films have attracted considerable attention due to the versatility of a sol–gel process for the fabrication of films on a wide range of substrates with tuneable compositions, physical properties and structures for commercial applications such as biosensors, biomedical and optical devices.[1–5] To prepare ultra-thin silica films on metal substrates, conventional deposition methods such as chemical vapour deposition[6] and physical vapour deposition[7–9] have mostly been used. Poor adhesion between silica and metal due to lack of chemical compatibility are major concerns in the metal processing and coating industries. To mitigate this problem, a layer of a transition metal or its oxide, several nanometres in thickness is often deposited to make a strong anchor between the oxide phase and a metal.[10]

An alternative approach to fabricate thin silica films are wet deposition methods in which silica precursors are hydrolyzed in solution followed by condensation and precipitation of silica particles in solution *via* sol–gel chemistry.[11] Silica particles are then deposited on a surface by dipping, spraying or spin-coating.[12–14] In general, sol–gel methods require acidic or basic pH conditions for synthesis and fabrication[7–14] unless required for the encapsulation of proteins[15] and cells[16] at physiological pH. In contrast, sponges and diatoms synthesise and fabricate precisely controlled and hierarchically order nano-structured silica materials from soluble silicon species under ambient conditions using special classes of proteins that include silicatein[17–20] and siliaffins.[21,22] To mimic biosilicification reaction *in vitro*, many synthetic polypeptides,[23–28] polyamines[29–33] and diblock polymers[34–36] have been synthesized and used to make silica particles in solution.

Similarly, several methods, for instance direct write assembly,[37] electrostatic deposition,[38–40] holographic patterning,[34] photolithography[41] and surface initiated polymerization,[42,43] have been used to fabricate silica films on polypeptide and polyamine coated solid substrates using a biomimetic approach. However, these methods have not proven to be useful for the fabrication of uniform silica films on a variety of substrates despite their being potential applications in the production of biosensor,[44,45] filter membranes[46] and structural materials.[47] In other studies using proteins to facilitate silica formation, Bovine serum albumin (BSA),[48] lysozyme[48,49] and silicatein[50–53] have been exploited to produce uniform inorganic films. His-tagged recombinant silicatein chemically tethered on nitrilotriacetic acid (NTA) terminated alkanethiol functionalized gold surfaces has been used to form heterogeneous silica, titania and zirconia films with uncontrolled thickness and roughness.[51–53] In our recent studies, we have shown that tuneable thickness (2–50 nm) and uniform silica films can be fabricated on polyamine (PAH, PEI and ODA) coated gold surfaces using microgram/cm^2 amounts of relatively cheap and readily available BSA and lysozyme.[48] We have also explored the ability of

School of Science and Technology, Nottingham Trent University, Clifton Lane, Nottingham, NG11 8NS, UK

† Electronic supplementary information (ESI) available. See DOI: 10.1039/c2jm15810h

nanomolar levels of silicatein covalently attached to glutardialdehyde-cystamine/cysteamine-Au surfaces to fabricate thin (maximum of 105nm for the best films) and uniform silica films with controlled physical properties.[50] However, this method required a three-step procedure to attach silicatein to the surface and required specificity of functionalization on those materials to be able to react with disulfide or thiol groups. Although this method was successful there is still a need for development of versatile immobilization strategies that would be applicable to a wide range of substrates.

Mussels, which are well-known for their ability to adhere to a wide variety of substrates such as metals, polymers, rocks and wood using adhesive proteins, are a source of inspiration for surface functionalization.[54,55] The adhesive properties of mussel adhesive proteins (MAPs) are due to the presence of L-3,4-dihydroxyphenylalanine (DOPA), a catecholic amino acid, that is formed by post-translational modification of tyrosine.[56,57] There are also specific amino acid decapeptide sequences such as (Ala-Lys-Pro-Ser-Tyr-DHP-Hyp-Thr-DOPA-Lys (DHP = dihydroxyproline)) repeated several times in the majority of MAPs.[58–60]

In this paper, we present a versatile and simple method to produce uniform silica films on Au, polystyrene and Si surfaces using nanomolar amounts of silicatein *via* the use of mussel adhesive protein inspired coatings. Silicatein was attached to substrates functionalized with DOPA or a DOPA containing peptide = Ala-Lys-Pro-Ser-Tyr-DHP-Hyp-Thr-DOPA-Lys utilising the polymerization to poly(DOPA) at alkaline pH (8.5) to form thin adherent films on the selected substrates.[61] The strong reactivity of the adsorbed films towards amine and thiol groups was exploited to attach silicatein to the surface *via* covalent interactions.[61,62] The thin films of poly(DOPA) or the decapeptide were found to act as "polymer cushions" that maintained the activity of silicatein by increasing the distance between the protein and the surface. Specific quantitative activity in silica formation could be correlated with maintenance of the protein secondary structures of silicatein.

Experimental details

Materials

Tetramethyl orthosilicate (TMOS) and DOPA were purchased from Sigma-Aldrich (Minneapolis, MN). Recombinant silicatein-α protein was purchased from BIOTECmarin (Germany) and was used as received. Citric acid/Na_2HPO_4 buffer (0.1 M, pH 4) and phosphate buffer (0.1 M, pH 7.2) was freshly prepared at 25 °C using citric acid and sodium salts of NaH_2PO_4 and Na_2HPO_4 obtained from Aldrich. Distilled deionized water with a conductivity of ~1 μS was used for all experiments.

Peptide synthesis

The DOPA containing decapeptide was synthesized using a solid phase peptide synthesis process as described in the literature.[62,63] In brief, the peptide was synthesized by Fmoc strategy with the following side chain protecting groups: t-butyl (Ser, Tyr, Hyp and Thr) and t-Boc (Lys). Fmoc deprotection was performed in 25% piperidine in N-methyl-2-pyrrolidinone (NMP) for 20 min. A preactivation step of 10 min was followed by a coupling reaction in NMP solution containing a mixture of Fmoc-amino acid: BOP:HOBt:DIEA (1 : 1 : 1 : 1) for 20 min. The synthesized decapeptide was cleaved from resin using 1 M TMSBr in TFA in the presence of thioanisole, m-cresol and EDT at 0 °C for 60 min. The decapeptide was further analyzed and purified using RP-HPLC. The estimated purity of the decapeptide was 96% (Fig. SI 1).

Protein immobilization study

Glass slides and Si wafers (111) were washed thoroughly with acetone and piranha solution (7 mL/3 mL mixtures of concentrated H_2SO_4 and 30% H_2O_2, respectively) for 30 min to remove any organic material and then rinsed with deionized water and dried before coating with gold using an Edwards sputter coater model S150B. Gold coated surfaces, polystyrene and Si wafers were immersed in 2 mg DOPA or DOPA containing peptide per 1 mL of 10 mM Tris buffer (pH 8.5) for 24 h to make thin films followed by rinsing with copious amounts of water to remove unbound DOPA and the DOPA containing peptide. Poly-(DOPA)/decapeptide coated gold, polystyrene and Si surfaces were transferred into silicatein (200 ng mL^{-1}, 8 nM) dissolved in citric acid/Na_2HPO_4 buffer (pH 4) solution for 3h. Aliquots of silicatein solution (50 μL) were removed at different times to measure the amount of non-immobilized silicatein *via* the fluorescamine assay[65] using a Tecan spectrafluor plate reader (360 nm excitation and 465 nm emission energy filters). The protein immobilized onto different surfaces and concentration per unit surface area (ng cm^{-2}) were calculated. The amount of decapeptide adsorbed on gold surfaces was also estimated using the fluorescamine assay.[65]

FTIR study

Infrared (ATR-FTIR) analysis of poly(DOPA)/decapeptide functionalized surfaces and silicatein bound surfaces was performed using a golden Gate attenuated total reflection (ATR) accessory in a Nicolet Magna IR-750 spectrophotometer continuously purged with dry air. Spectra were recorded at 4 cm^{-1} resolution with 1026 scans being averaged and then smoothed by 11 point adjacent averaging.

Fabrication and analysis of silica films

100 mM TMOS solution was hydrolyzed with 1 mM HCl for 15 min. After 15 min, a known volume of phosphate buffer was added to the hydrolyzed TMOS to raise the pH to 7.2. Silicatein coated surfaces and control surfaces were dipped vertically in hydrolyzed, buffered TMOS solution for 2 h, rinsed with water and dried under a stream of N_2 gas. ATR-FTIR analysis was performed to investigate the formation of silica films on various surfaces.

Measurement of immobilized silicatein activity

To assess the activity of immobilized silicatein, unconsumed hydrolyzed TMOS remaining in solution after removal of surfaces (after silica film fabrication) were treated with 2 M NaOH for 1 h at 80 °C to completely break down all silica species into monomer and dimer. The concentration of silicic acid in

solution was then estimated by the molybdenum blue colorimetric method described by Iler.[66] In brief, aliquots of 10 μL solution were removed from different samples and added to solutions containing 15 mL of water and 1.5 mL of an acidic solution of ammonium molydate followed by incubation of the resulting solutions for 20 min at room temperature. A reducing agent containing Metol (8mL) was then added to each solution, and the absorbance of the blue silicomolybdate complex was measured after 2 h of reaction at 810 nm using a Unicam UV2 UV-vis spectrophotometer. Similarly the amount of silicic acid consumed in synthesis of silica particles in solution (100 mM prehydrolyzed TMOS was reacted with 200 ng mL^{-1} silicatein for 2 h) were estimated. Samples were centrifuged and the precipitated silica particles washed three times to remove free hydrolyzed TMOS. Silica particles were broken down to monomer/dimer using 2 M NaOH as described above. The concentration of silicic acid consumed in this process was estimated to be 16.2 ± 2 mM. The specific activity of free silicatein in solution was considered as 100% to estimate the specific activity of immobilized silicatein on various surfaces.

Inductively coupled plasma-optical emission spectroscopy (ICP-OES) measurement of silica release from films

ICP-OES was conducted using a Perkin Elmer Optima 2100 DV Optical Emission Spectrometer using WinLab32 software. Silicon content was estimated by measuring signal intensity at 251.611 nm against a standard curve of between 0.01 and 0.75 mg L^{-1} orthosilicic acid in phosphate buffer (pH 7.2). Silica coated surfaces were incubated with phosphate buffer (pH 7.2) for 24 h to leach free silica particles from the films. The resulting phosphate buffer solutions were treated with 2 M NaOH at 80 °C for 1 h to convert any condensed silica into silicic acid. Silica concentration was measured from 100 μL aliquots following the method described by Belton *et al.*[30]

Atomic force microscopy study

Poly(DOPA), decapeptide, silicatein, and silica coated surfaces were analyzed by atomic force microscopy (AFM) in non-contact mode using a Pacific Nanotechnology Nano-R2 instrument with SiN probes at a scan rate of 0.5 Hz, in air. The line profile analysis of different surfaces was performed to estimate the thickness of protein and silica films after all stages of the film formation process were complete. The roughness of the surface was assessed by measuring roughness parameters (Rrms, root-mean-square roughness) using Nanorule.exe software supplied with the instrument.

Scanning electron microscopy study

Silica coated surfaces were mounted on aluminium stubs with double-sided adhesive carbon tape and coated with palladium/gold before analysing using a JEOL JSM 7400F FE instrument operated at an accelerated voltage of 20 kV.

Result and discussion

The aim of this study was to develop versatile methods for the immobilization of silicatein on a variety of surfaces in order to fabricate uniform silica films. In a previous publication, a three-step procedure was used in which a bifunctional molecule (thickness of film, 1.1 nm) was coated on gold surfaces before silicatein was adsorbed *via* covalent interactions.[50] In this current contribution, mussel adhesive protein inspired films were formed on variety of surfaces prior to silicatein immobilization with improved activity of silicatein (Scheme 1). All surfaces tested were amenable to the deposition protocol and for brevity the detailed results for the formation of silica films on a gold surface are described.

The deposition of the decapeptide was performed at a range of different pH values to optimise coating. As an example, the amount of deposited decapeptide on the gold surface at pH 8.5 was calculated to be 2000 ± 235 ng cm^{-2}, higher than that obtained at pH 6.5 (800 ± 110 ng cm^{-2}) due to the fact that the DOPA molecule does not interact strongly with the gold surface *via* the gold-catechol bond at pH 6.5.[62] In addition, a single DOPA residue in the peptide does not promote strong adsorption of the decapeptide on the gold surface at pH 6.5. It is likely that other residues in the decapeptide play an important role in the adhesion process at pH 6.5.[64,67] Gold surfaces coated at pH 8.5 were used for further study.

The deposition of a thin layer of poly(DOPA) and poly(decapeptide) on gold surfaces at pH 8.5 was analysed by ATR-FTIR. Curve 2, Fig. 1A, corresponds to the FTIR spectrum of poly(DOPA), showing the C=C stretching vibration at 1590 cm^{-1} and catechol ring vibration between 1300 and 1140 cm^{-1}. The O–H stretching vibration of poly(DOPA) was observed between 3600–3300 cm^{-1} (an inset of curve 2, Fig. 1A).[67] No signal arising from amine or carbonyl bonds was observed on a plain gold surface (Curve 1, Fig. 1A). The deposition of the film is initiated by oxidation of DOPA molecules on the gold surface followed by polymerization in a manner similar to melanin formation.[61,68] The observed colour change of the reaction solution from light pink to dark blue during the DOPA coating process also indicates polymerization occurring on the gold surface, data not shown. DOPA forms strong covalent and non-covalent interactions with the gold surface though the formation of Au-catechol bonds,[62] however, the exact polymerization mechanism of DOPA is not know so far. Curve 2 shows the

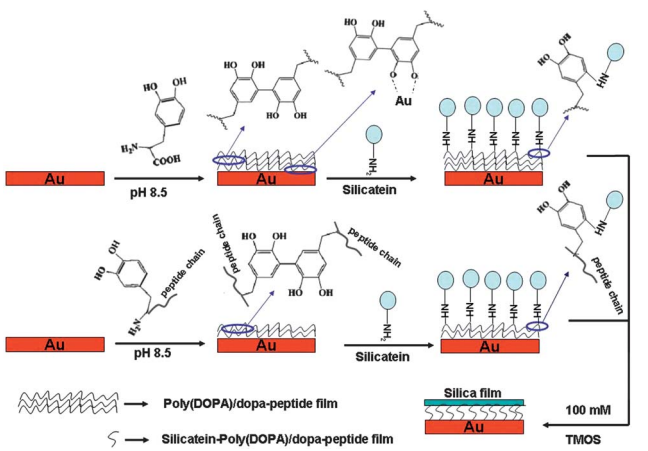

Scheme 1 Representation of the stepwise coating of a substrate (note that the scheme is not to scale).

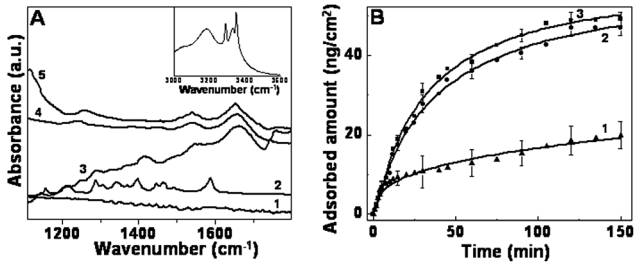

Fig. 1 **(A)** FTIR spectra of bare gold surface (curve 1), poly(DOPA)-Au (curve 2), decapeptide-Au (curve 3), silicatein-poly(DOPA)-Au (curve 4) and silicatein-decapeptide-Au surface (curve 5). An inset of (A) shows the FTIR spectrum of poly(DOPA) in the 3000–3600 cm^{-1} region. **(B)** Time dependent immobilization of silicatein on a bare gold surface (curve 1), polydecapeptide-Au (curve 2) and poly(DOPA)-Au (curve 3) surfaces.

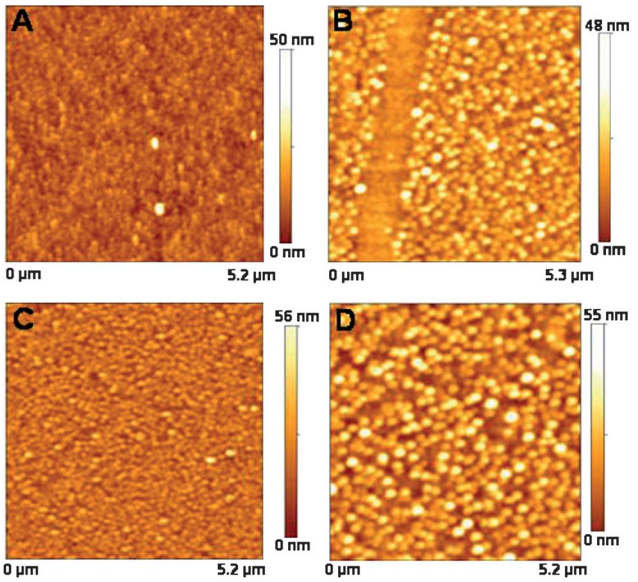

Fig. 2 Representative AFM images of poly(DOPA)-Au (A), decapeptide-Au (B), silicatein-poly(DOPA)-Au (C) and silicatein-decapeptide-Au surface (D).

distinct signals arising from amide groups at 1650 and 1555 cm^{-1} along with bending and stretching vibrations from phenolic C–O–H at 1378 and 1290 cm^{-1} respectively, for DOPA indicating the deposition of the decapeptide on the gold surface (Curve 2, Fig. 1A).[67] AFM analysis provided supporting information with the formation of uniform layers of poly(DOPA) and decapeptide with thickness of 25 ± 2 and 22 ± 1.3 respectively on the gold surface after incubation for 24 h (Table 1 and Fig. 2A and B).

The adsorption behaviour of silicatein on a plain gold surface, poly(DOPA) and decapeptide coated gold surfaces is presented in Fig. 1B. A small amount of silicatein was adsorbed on a plain gold surface due to non-specific physical interactions after 3 h of incubation which led to the formation of heterogeneous silicatein films (Table 1 and Fig. 1B and SI 2A). In contrast, a large amount of silicatein (49 ng cm^{-2}) was adsorbed on poly(DOPA) and decapeptide coated gold surfaces (Table 1 and Fig. 1B) as compared to our previous study where 28 ng cm^{-2} of silicatein was adsorbed on the cystamine-glutardialdehyde-Au surface.[50] In this process, poly(DOPA) and decapeptide films with thickness of 25 and 22 nm respectively introduced enough space between the adsorbed silicatein and the gold surface to improve the strength of adsorption of the silicatein with maintenance of its activity. Polydopamine exhibits a strong reactivity toward amine and thiol groups[61,62] and the deposited poly(DOPA) coating contains both catechol and quinone functional groups with the latter being capable of covalent coupling with protein through a reaction between poly(DOPA) and positively charged protein molecules (Scheme 1).[69] A previous study has shown that catechol and quinone groups were in equilibrium at pH 7, with the equilibrium shifted toward the quinone form under alkaline conditions such as used in this study, leading to a strong adsorption of protein.[69] The adsorption behaviour of silicatein appeared to exhibit multiple steps of adsorption on poly(DOPA) and decapeptide coated surfaces and was fitted using the Freundlich isotherm.[50] Freundlich constants k and n are related to the adsorption rate constant and the estimation of intensity of adsorption respectively. When the value of $n < 1$ or >1, this implies that the adsorption process arises from chemical or physical processes respectively. n1 and n2 were calculated from the initial phase (0–60 min) and late phase adsorption of silicatein (60–120 mins) respectively for the different surfaces (data not shown). Silicatein adsorbed on poly(DOPA) and decapeptide coated surface through covalent coupling[61,62,69] ($n1 < 1$) in the initial phase followed by physical adsorption ($n2 > 1$) during the late phase of the reaction, leading to the deposition of more than a monolayer of silicatein (Table 1). In contrast, on the bare gold surface silicatein adsorbed *via* physical adsorption only (n1 and $n2 > 1$) (Table 1).

Silicatein adsorbed uniformly on both poly(DOPA) and decapeptide coated gold surfaces as observed by AFM (Fig. 2C

Table 1 Estimation of amount of protein adsorbed, rate constant, Freundlich constants (n1 and n2), silicic acid consumed, and thickness/roughness of films formed at different coating stages on the gold surfaces

Surface	Au	Poly (DOPA)-Au	Decapeptide-Au	Silicatein-Poly(DOPA)-Au	Silicatein-decapeptide-Au	Silicatein-Au
Silicatein immobilized (ng cm^{-2})	18 ± 3.3	49 ± 1.8	46 ± 2.1			
Rate constant k (min^{-1})				6.7×10^{-3}	7.1×10^{-3}	1.1×10^{-4}
n1 (min^{-1})				0.842	0.892	1.22
n2 (min^{-1})				2.57	3.37	1.94
Thickness (nm)	5 ± 0.5	25 ± 2	22 ± 1.3	29.2 ± 1.2	28 ± 1	8.9 ± 1.1
Roughness (nm)	0.4 ± 0.1	2.64 ± 0.89	3.9 ± 1.7	3.15 ± 2.2	4.3 ± 1.65	3.4 ± 1.23
Amount of silicic acid consumed (mM)	0	0	0	16.4 ± 2	14.5 ± 1.3	1.67 ± 1.2

and D). Measurement of thickness and roughness at each stage of the coating process showed an increase in thickness and roughness of films with distinct layers being formed at each stage (Table 1). This result was commensurate with FTIR spectral data, which showed the characteristic signals of amide I and II bands of silicatein obtained from both surfaces (Curves 4 and 5, Fig. 1A). The combined thickness of silicatein-poly(DOPA) and silicatein-decapeptide is 29.2 ± 1.2 and 28 ± 1 nm respectively. The diameter of the 28 kDa globular protein is approximately 3.2 nm, indicating the deposition of more than a monolayer of silicatein on both surfaces (Table 1). The amount of protein adsorbed is approximately the same although the thickness of the silicatein film is slightly less on the decapeptide surface (Table 1), which could have arisen through the diffusion of some silicatein molecules inside the peptide coating and rearrangement of the protein on the decapeptide-Au surface.[70,71] Support for this hypothesis comes from the observation that the silicatein-decapeptide surface was more rough than the silicatein-poly-(DOPA)-Au surface (Table 1).

To confirm the activity of covalently attached silicatein, silicatein coated surfaces were used for the fabrication of silica films at ambient conditions by treating both surfaces (silicatein-poly(DOPA)-Au and silicatein-decapeptide-Au) and a plain gold surface with prehydrolysed TMOS solution. No silica films were observed on a bare gold surface after 2 h of treatment, in good agreement with FTIR data, which does not show any signal for Si–O stretching vibrations in the characteristic 1100–800 cm^{-1} region (Curve 1, Fig. 4A and Fig. SI 2B). Uniform silica films were deposited on silicatein-poly(DOPA)-Au and silicatein-decapeptide-Au surfaces in comparison with an heterogeneous film formed on silicatein-Au surface, demonstrating the significance of functionalization of the gold surface prior to silicatein immobilization for optimisation of activity (Fig. 3A and B and Fig. SI 2C). Spherical silica particles of size from 20–30 nm were formed and interconnected with each other on both surfaces to form uniform silica films (Fig. 3A and B). FTIR analysis showed the characteristic vibrational signals of silica at ~1040, 950 and 800 cm^{-1}, corresponding to Si–O–Si (asym), Si–OH and Si–O–Si (sym) bonds respectively (Curves 4 and 5, Fig. 4A), indicating the presence of silica on these surfaces. In control experiments, no formation of silica films were observed when precipitation of silica was performed on poly(DOPA)-Au and decapeptide-Au surfaces without silicatein even after 2 h of reaction (Fig. 3C and D and curves 2 and 3, Fig. 4A). Silica films can be fabricated on poly(DOPA) coated surfaces in an economical fashion compared to the more expensive decapeptide coated surface, although both surfaces produce a similar quality of silica film.

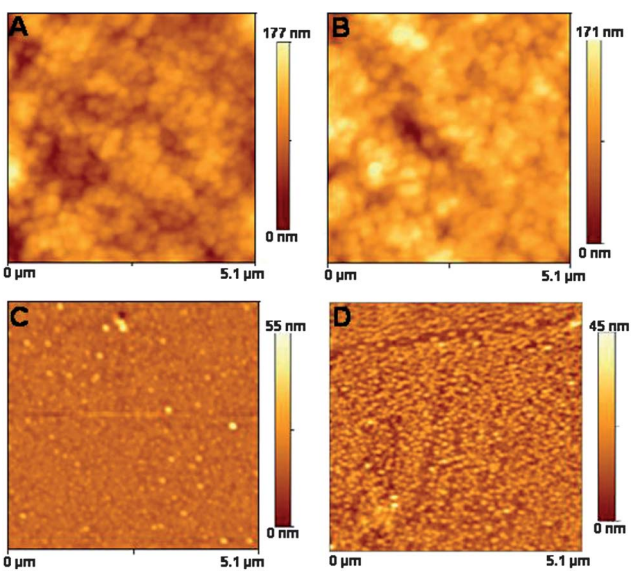

Fig. 3 Representative AFM images of silica films on silicatein-poly-(DOPA)-Au (A) and silicatein-decapeptide-Au (B), poly(DOPA)-Au (C), decapeptide-Au surface (D).

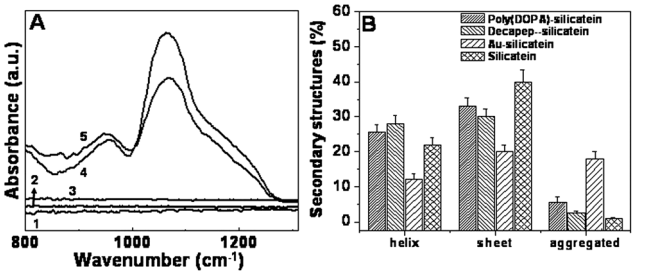

Fig. 4 **(A)** FTIR spectra of silica films deposited on a bare gold surface (curve 1), poly(DOPA)-Au (curve 2), decapeptide-Au (curve 3), silicatein-poly(DOPA)-Au (curve 4) and silicatein-decapeptide-Au surface (curve 5). **(B)** Secondary structures analysis of silicatein adsorbed on various surfaces. It should be noted that only estimated helix, sheet and aggregated secondary structures from curve-fitting analysis are shown in the figure.

The two coatings were found to differ in their ability to support silicatein adsorption/silica formation after storage. Poly-(DOPA) coated surfaces stored at room temperature were active for at least 30 days compared to the decapeptide coated surface which lost virtually all activity for silicatein binding and subsequent silica formation after storage at room temperature for 5 days (Fig. SI 3). Activity of the DOPA containing decapeptide was retained for at least 5 days if surfaces were stored at 4–8 °C (Fig. SI 3).

A molybdenum blue assay was performed to estimate the amount of silicic acid used in the formation of silica films. 6.85 ± 0.82 and 6.44 ± 0.96 mM cm^{-2} silicic acid were consumed by the adsorbed silicatein during silica film formation with the combined thickness of 134 ± 6 and 106 ± 8 nm and roughness of 4.52 ± 0.45 and 3.67 ± 0.39 nm cm^{-2} on silicatein-poly(DOPA)-Au and silicatein-decapeptide-Au surfaces respectively. The variation of thickness on both surfaces suggests that silicatein diffused inside the decapeptide layer does not recognise the presence of hydrolyzed TMOS and only silicatein molecules present on the surface take part in condensation reactions, leading to a lower consumption of silicic acid and the formation of thinner silica films (106 nm). These results confirm that the catalytic activity of silicatein (*ca.* 95%) was maintained after adsorption on both surfaces compared to 100% activity for silicatein in solution, however, a low level (0.74 ± 0.3 mM cm^{-2}) of silicic acid consumption was found on silicatein-Au surfaces perhaps due to the denaturation of the adsorbed silicatein.[50] In a comparison with our previous deposition studies using the more complex process,[50] 4.32 mM cm^{-2} of silicic acid was

consumed by 28 nm cm^{-2} of chemically tethered silicatein on the gold surface to form silica films with thickness and roughness of 105 nm and 5.2 nm cm^{-2} respectively, indicating that the thicker silica film has a higher tendency to form a less rough surface compared to the thinner film.

To determine the silica film robustness, the silica films were incubated in phosphate buffer (pH 7.2) for 24 h. ICP-OES measurement showed that 1.4 ± 0.1 and 1.2 ± 0.11 μM silica, (*ca.* 0.015% of that condensed on the surface) was removed from the surface over the 24 h period suggesting that the films formed were stable or that only a very small number of silica particles settled on the surfaces during the drying process were leached from the surfaces during the incubation period.

Secondary structural analysis of silicatein after adsorption on the gold surface by analysis of the amide I and II band shapes suggests that an increase in the aggregated structures observed during AFM analysis on a plain gold surface (Fig. SI 2A) can be related to a reduction of α-helix and β-sheet structures as compared to other surfaces (Fig. 4B).[72] For the poly(DOPA) and decapeptide coated surfaces, higher levels of α-helix (*ca.* 23%) and β-sheet (*ca.* 33%) secondary structures, characteristic of the presence of active silicatein were observed (Fig. 4B and SI 4).[72,73] This observation correlates well with studies of the structure of Cathepsin L, which has a very similar amino acid sequence to silicatein with 20 β-sheet structures and 10 α-helices.[72,73] We believe that thicker layers of poly(DOPA) and of the decapeptide act as "polymer cushions" that nullify the effect of a plain gold surface on conformational changes of adsorbed silicatein. The specific activity of silicatein on both surfaces was measured to be 95% in comparison with the activity of free silicatein found in solution, whose activity was considered as 100%. The slightly lower level of β-sheet structures and unavailability of silicatein molecules present within the multilayer films led to reduction in activity of adsorbed silicatein on both surfaces in comparison with the activity in solution.[50]

Many inorganic and organic substrates (Ag, Cu, SiO_2, polystyrene and polycarbonate) can be modified with poly(DOPA) coatings.[61] For a range of applications such as biosensors, biomedical devices and in tissue engineering, silica films need to be easily fabricated on polystyrene and silicon substrates over multiple length scales. As exemplars of our approach, uniform silica films were prepared on a range of substrates (polystyrene and silicon). The substrates were functionalized with poly(DOPA) as described above. Thin and uniform films of silica were fabricated on these surfaces, which were chemically tethered with silicatein (Fig. 5). The thickness of the silica films (100 nm) was similar to the films fabricated on the gold surface, implying the attached silicatein was also active on these surfaces. Low magnification SEM images show that uniform and smooth silica films can be prepared over surface areas more than 1 cm^2 although a few silica particles were observed on these surfaces that had adventitiously deposited during the synthesis (Fig. 5B and D).

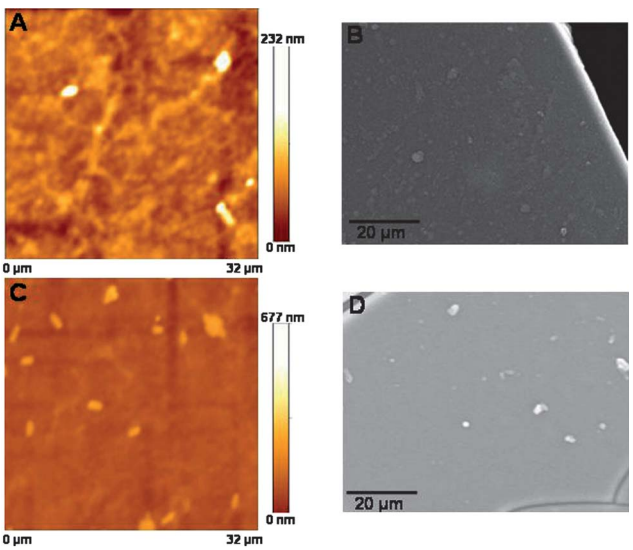

Fig. 5 AFM and SEM analysis of silica films fabricated on polystyrene (A and B) and Si wafer (C and D).

Summary

We have shown a robust and versatile method for the fabrication of uniform silica films on poly(DOPA) and decapeptide coated substrates (Au, polystyrene and Si) using nanogram amounts of silicatein under environmentally friendly conditions. The strong adhesive property of DOPA and the decapeptide under mildly alkaline conditions was exploited to functionalize the gold surface to achieve a large amount of adsorption of silicatein with its activity maintained. The native α-helix and β-sheet secondary structures of silicatein predominantly present on the thicker films of poly(DOPA) and decapeptide on the gold surfaces as compared to a plain gold surface play an important role in maintaining the native state and the activity of silicatein. The estimated specific activity of adsorbed silicatein and the formation of uniform silica films on these surfaces confirm that the active site of silicatein was oriented towards silicic acid species present in solution. As similar results for silica formation are obtained on both surfaces, DOPA can be used instead of the specific decapeptide for fabrication of stable silica films. This two-step method of silicatein adsorption is distinctive in its use of simple ingredients and its ease of uniform silica film fabrication under ambient reaction conditions makes this procedure potentially economically applicable for the fabrication of inorganic films on a variety of surfaces over multiple length scales.

References

1 D. K. Kambhampati, T. A. M. Jakob, J. W. Robertson, M. Cai, J. E. Pemberton and W. Knoll, *Langmuir*, 2001, **17**, 1169–1175.
2 I. Ruach-Nir, T. A. Bendikov, I. Doron-Mor, Z. Barkay, A. Vaskevich and I. Rubinstein, *J. Am. Chem. Soc.*, 2007, **129**, 84–92.
3 M. Cai and J. E. Pemberton, *Fresenius J. Anal. Chem.*, 2001, **369**, 328–334.
4 G. Sun and G. Grundmeier, *Thin Solid Films*, 2006, **515**, 1266–1274.
5 L. Giordano, F. Cinquini and G. Pacchioni, *Phys. Rev. B: Condens. Matter Mater. Phys.*, 2005, **73**, 045414–045416.
6 X. G. Zhang, *Electrochemistry of Silicon and Its Oxide*; Kluwer Academic/Plenum Publishers: New York, 2001; pp 91–130.
7 A. P. Legrand, *The Surface Properties of Silicas*; John Wiley & Sons: Chichester, U.K., 1998; pp 6–7.
8 E. F. Vansant, P. Van Der Voort, K. C. Vrancken, *Characterization and Chemical Modification of the Silica Surface*; Elsevier: Amsterdam, 1995; Vol. 93, pp 66–67.
9 P. Lundgren, M. O. Andersson, K. R. Farmer and O. Engstrom, *Microelectron. Eng.*, 1995, **28**, 67–70.

10 P. Macech and J. E. Pemberton, *Langmuir*, 2007, **23**, 9816–9822.
11 M. Cai, M. Ho and J. E. Pemberton, *Langmuir*, 2000, **16**, 3446–3453.
12 W. R. Thompson and J. E. Pemberton, *Anal. Chem.*, 1994, **66**, 3362–3370.
13 W. R. Thompson and J. E. Pemberton, *Chem. Mater.*, 1995, **7**, 130–136.
14 G. Sun and G. Grundmeier, *Thin Solid Films*, 2006, **515**, 1266–1274.
15 L. Betancor and H. R. Luckarift, *Trends Biotechnol.*, 2008, **26**, 566–572.
16 G. Carturan, R. D. Toso, S. Boninsenga and R. D. Monte, *J. Mater. Chem.*, 2004, **14**, 2087.
17 K. Shimizu, J. Cha, G. D. Stucky and D. E. Morse, *Proc. Natl. Acad. Sci. U. S. A.*, 1998, **95**, 6234–6238.
18 N. Kroger, R. Deutzmann, C. Bergsdorf and M. Sumper, *Proc. Natl. Acad. Sci. U. S. A.*, 2000, **97**, 14133–14338.
19 Y. Zhou, K. Shimizu, J. N. Cha, G. D. Stucky and D. E. Morse, *Angew. Chem., Int. Ed.*, 1999, **38**, 779–782.
20 J. Cha, K. Shimizu, Y. Zhou, S. C. Christiansen, B. F. Chmelka, G. D. Stucky and D. E. Morse, *Proc. Natl. Acad. Sci. U. S. A.*, 1999, **96**, 361–365.
21 N. Kroger, R. Deutzmann and M. Sumper, *Science*, 1999, **286**, 1129–1132.
22 M. S. Kent, J. K. Murton, F. J. Zendejas, H. Tran, B. A. Simmons, S. Sajita and I. Kuzmenko, *Langmuir*, 2009, **25**, 305–310.
23 E. G. Bellomo and T. J. Deming, *J. Am. Chem. Soc.*, 2006, **128**, 2276–2279.
24 T. Coradin and J. Livage, *Colloids Surf., B*, 2001, **21**, 329–336.
25 M. R. Knecht and D. W. Wright, *Chem. Commun.*, 2003, 3038–3039.
26 R. R. Naik, L. L. Brott, S. J. Clarson and M. O. Stone, *J. Nanosci. Nanotechnol.*, 2002, **2**, 95–100.
27 S. V. Patwardhan, N. Mukherjee, M. Steinitz-Kannan and S. J. Clarson, *Chem. Commun.*, 2003, 1122–1123.
28 M. M. Tomczak, C. Lawrence, L. F. Drummy, L. A. Sowards, D. C. Glawe, M. O. Stone, C. C. Perry, D. J. Pochan, T. J. Deming and R. R. Naik, *J. Am. Chem. Soc.*, 2005, **127**, 12577–12582.
29 D. Belton, G. Paine, S. V. Patwardhan and C. C. Perry, *J. Mater. Chem.*, 2004, **14**, 2231–2241.
30 D. Belton, S. V. Patwardhan and C. C. Perry, *J. Mater. Chem.*, 2005, **15**, 4629–4638.
31 D. Belton, S. V. Patwardhan and C. C. Perry, *Chem. Commun.*, 2005, 3475–3477.
32 A. Bernecker, R. Wieneke, R. Riedel, M. Seibt, A. Geyer and C. Steinem, *J. Am. Chem. Soc.*, 2010, **132**, 1023–31.
33 D. Belton, S. V. Patwardhan, V. V. Annekov, E. N. Danilovtseva and C. C. Perry, *Proc. Natl. Acad. Sci. U. S. A.*, 2008, **105**, 5963–5968.
34 L. L. Brott, R. R. Naik, D. J. Pikas, S. M. Kirkpatrick, D. W. Tomlin, P. W. Whitlock, S. J. Clarson and M. O. Stone, *Nature*, 2001, **413**, 291–293.
35 H. Menzel, S. Horstmann, P. Behrens, P. Barnreuther, I. Kruger and M. Jahns, *Chem. Commun.*, 2003, 2994–2995.
36 J. N. Cha, G. D. Stucky, D. E. Morse and T. J. Deming, *Nature*, 2000, **403**, 289–292.
37 M. Xu, G. M. Gratson, E. B. Duoss, R. F. Shepherd and J. A. Lewis, *Soft Matter*, 2006, **2**, 205–209.
38 D. D. Glawe, F. Rodriguez, M. O. Stone and R. R. Naik, *Langmuir*, 2005, **21**, 717–720.
39 S. D. Pogula, S. V. Patwardhan, C. C. Perry, J. W. Gillespie, S. Yarlagadda and K. L. Kick, *Langmuir*, 2007, **23**, 6677–6683.
40 N. Laugel, J. Hemmerle, C. Porcel, J.-C. Voegel, P. Schaaf and V. Ball, *Langmuir*, 2007, **23**, 3706–3711.
41 E. A. Coffman, A. V. Melechko, D. P. Allison, M. L. Simpson and M. J. Doktycz, *Langmuir*, 2004, **20**, 8431–8436.
42 D. J. Kim, K. B. Lee, Y. S. Chi, W. J. Kim, H. J. Paik and I. S. Choi, *Langmuir*, 2004, **20**, 7904–7906.
43 D. J. Kim, K. B. Lee, T. G. Lee, H. K. Shon, W. J. Kim, H. J. Paik and I. S. Choi, *Small*, 2005, **1**, 992–996.
44 S. A. Grant and R. S. Glass, *IEEE Trans. Biomed. Eng.*, 1999, **46**, 1207–1211.
45 H. Schmidt, *J. Sol-Gel Sci. Technol.*, 2006, **40**, 115–130.
46 A. Stein, B. J. Melde and R. C. Schroden, *Adv. Mater.*, 2000, **12**, 1403.
47 R. A. Caruso and M. Antonietti, *Chem. Mater.*, 2001, **13**, 3272–3282.
48 A. Rai and C. C. Perry, *Silicon*, 2010, **1**, 91–101.
49 H. R. Luckarift, S. Balasubramanian, S. Paliwal, G. R. Johnson and A. L. Simonian, *Colloids Surf., B*, 2007, **58**, 28–33.
50 A. Rai and C. C. Perry, *Langmuir*, 2010, **26**, 4152–4159.
51 M. N. Tahir, M. Eberhardt, H. A. Therese, U. Kolb, P. Theato, W. E. G. Muller, H. C. Schroder and W. Tremel, *Angew. Chem., Int. Ed.*, 2006, **45**, 4803–4809.
52 M. N. Tahir, P. Theato, W. E. G. Muller, H. C. Schroder, A. Borejko, S. Faiss, A. Janshoff, J. Huth and W. Tremel, *Chem. Commun.*, 2005, 5533–5535.
53 M. N. Tahir, P. Theato, W. E. G. Muller, H. C. Schroder, A. Janshoff, J. Jhang, J. Huth and W. Tremel, *Chem. Commun.*, 2004, 2848–2849.
54 J. H. Waite, *Chemtech.*, 1987, **17**, 692–697.
55 G. A. Young, D. J. Crisp, in *Adhesion*, Allen, K. W.; Ed.; Applied Science, London, vol. 6, 1982.
56 J. H. Waite and M. L. Tanzer, *Science*, 1981, **212**, 1038–1040.
57 J. H. Waite and M. L. Tanzer, *Biochem. Biophys. Res. Commun.*, 1980, **96**, 1554–1561.
58 H. Yamamoto, *Biotechnol. Genet. Eng. Rev.*, 1996, **13**, 133–165.
59 J. H. Waite, T. J. Housley and M. L. Tanzer, *Biochemistry*, 1985, **24**, 5010–5014.
60 R. A. Laursen, *In Structure, Cellular Synthesis and Assembly of Biopolymers*; Case, S. T.; Ed.; Springer-Verlag, 1992; pp 55.
61 H. Lee, S. M. Dellatore, W. M. Miller and P. B. Messersmith, *Science*, 2007, **318**, 426–430.
62 H. Lee, N. F. Schere and W. M. Messersmith, *Proc. Natl. Acad. Sci. U. S. A.*, 2006, **103**, 12999–13003.
63 B. H. Hu and P. B. Messersmith, *Tetrahedron Lett.*, 2000, **41**, 5795–5798.
64 J. L. Dalsin, B. H. Hu, B. P. Lee and P. B. Messersmith, *J. Am. Chem. Soc.*, 2003, **125**, 4253–4258.
65 S. Underfriend, S. Stein, P. Bohlen, W. Dairman, W. Leimgruber and M. Weigele, *Science*, 1972, **178**, 871–872.
66 R. K. Iler, *The Chemistry of Silica*, John Wiley & Sons, New York, 1979.
67 Z. Y. Xi, Y. Y. Xu, L. P. Zhu, Y. Wang and B. K. Zhu, *J. Membr. Sci.*, 2009, **327**, 244–253.
68 F. Bernmann, A. Ponche, C. Ringwald, J. Hemmerle, J. Raya, B. Bechinger, J. C. Voegel, P. Schaaf and V. Ball, *J. Phys. Chem. C*, 2009, **113**, 8234–8244.
69 H. Lee, J. Rho and P. B. Messersmith, *Adv. Mater.*, 2009, **21**, 431–434.
70 D. M. Hylton, D. Klee, M. Fabry and H. Hocker, *J. Colloid Interface Sci.*, 1999, **220**, 198–204.
71 M. Kleijn and W. Norde, *Heterog. Chem. Rev.*, 1995, **2**, 157–172.
72 S. V. Patwardhan, S. A. Holt, S. M. Kelly, M. Kreiner, C. C. Perry and C. F. Van der walle, *Biomacromolecules*, 2010, **11**, 3126–3135.
73 G. Croce, A. Frache, M. Milanesio, L. Marchese, M. Causa, D. Viterbo, A. Barbaglia, V. Bolis, G. Bavestrello, C. Cerrano, U. Benatti, M. Pozzolini, M. Giovine and H. Amenitsch, *Biophys. J.*, 2004, **86**, 526–534.